IUCrJ
ISSN 2052-2525
CHEMISTRY | CRYSTENG

Functional materials design: octahedral tilts in hybrid n = 1 Ruddlesden–Popper phases

Emma E. McCabe*

Durham University, Lower Mountjoy, South Road, Durham, DH1 3LE, United Kingdom. *Correspondence e-mail: emma.mccabe@durham.ac.uk

Keywords: perovskites; symmetry mode analysis; organic–inorganic hybrid materials; Ruddlesden–Popper structure.

The importance of hybrid perovskites and more recently their layered analogues [*e.g.* the high efficiency and stable Ruddlesden–Popper (RP) phases (Stoumpos *et al.*, 2016; Tsai *et al.*, 2016)] is undisputed with significant research resources dedicated to these functional materials. Recently several excellent studies of the structural chemistry of hybrid layered perovskite-related materials have been published (Saparov & Mitzi, 2016; Mao *et al.*, 2019) including an in-depth exploration by McNulty and Lightfoot of several families of layered hybrid perovskite-related materials (McNulty & Lightfoot, 2021). Understanding the precise structure (and symmetry) of these systems is essential for designing and optimizing functional materials, but until recently, there have been few studies on specific families: Li *et al.* provide an interesting comparison of hybrid Dion–Jacobson materials (Li *et al.*, 2019) with their all-inorganic analogues (Aleksandrov & Bartolomé, 2001), but the n = 1 RP family has not received a systematic crystallographic investigation until now. In this issue of **IUCrJ**, Liu *et al.* take on this challenge with gusto, mapping out the structures expected for the hybrid n = 1 RP materials (Liu *et al.*, 2023). This builds on the excellent work of McNulty & Lightfoot (2021), but by focusing on only a single family, Liu *et al.* can identify specific drivers for tilts and structure types, and even go some way to providing a blueprint for designing hybrid n = 1 RP phases with targeted symmetries.

In order to fully appreciate the authors' work, it is useful to briefly consider the wider field of structural chemistry of perovskites (and related phases). The mineral perovskite, $CaTiO_3$, named after Count Perovski, gives its name to this structure type and well known family of materials (Attfield *et al.*, 2015). Perovskites have long been an important research focus, from the all-inorganic phases [*e.g.* ferroelectric $BaTiO_3$ (Megaw, 1952)] to the recent 'hybrid' perovskites [*e.g.* $CH_3NH_3PbI_3$ (Kojima *et al.*, 2009)] known for their impressive photovoltaic properties (NREL, 2023). With the general formula ABX_3 (A, B are cations; X are anions), the typical perovskite structure can be described in terms of cubic-close-packed AX_3 layers with smaller B cations in between (West, 2014) to give the familiar three-dimensional network of corner-linked BX_6 octahedra [Fig. 1(*a*)]. What makes the perovskite family of materials so important is their compositional flexibility: this allows the design of functional perovskite materials with a huge range of properties.

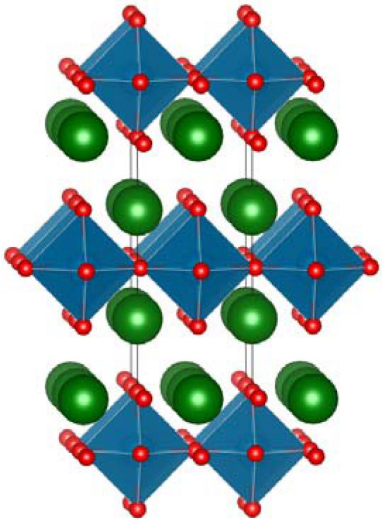

The relatively simple topology of corner-linked BX_6 shown in Fig. 1(*a*) belies the rich structural complexity of this family: the arisotype structure is of $Pm\bar{3}m$ symmetry, but few materials adopt this ideal structure and several types of distortion (driven by geometric or electronic factors) are possible (Salje *et al.*, 1989). An important type of distortion involves rotation of essentially rigid BX_6 octahedra (Glazer, 1972; Howard & Stokes, 1998; Woodward, 1997) to optimize bonding for the various ions. The resulting change in structure (and symmetry) has an enormous impact on properties and so tuning these rotations has been a powerful method of optimizing properties.

Alongside the perovskite with its three-dimensional connectivity of BX_6 octahedra, several families of perovskite-related materials with layered structures are known, including the RP (Ruddlesden & Popper, 1957, 1958) and Aurivillius families (Aurivillius, 1950*a*,*b*, 1952) [Figs. 1(*b*), 1(*c*)]. The connectivity of BX_6 octahedra is maintained in two dimensions, but perovskite blocks are separated along the third direction by either AX rocksalt layers (for the RP phases) or by fluorite-like $[Bi_2O_2]^{2+}$ layers for the Aurivillius phases. As for the ABX_3 perovskites, these phases readily undergo distortions from their aristotype structures (of $I4/mmm$ symmetry) involving rotations of the BX_6 octahedra. These have been systematically explored in the context of all-inorganic materials (Aleksandrov & Bartolome, 1994; Aleksandrov & Bartolomé, 2001; Hatch & Stokes,

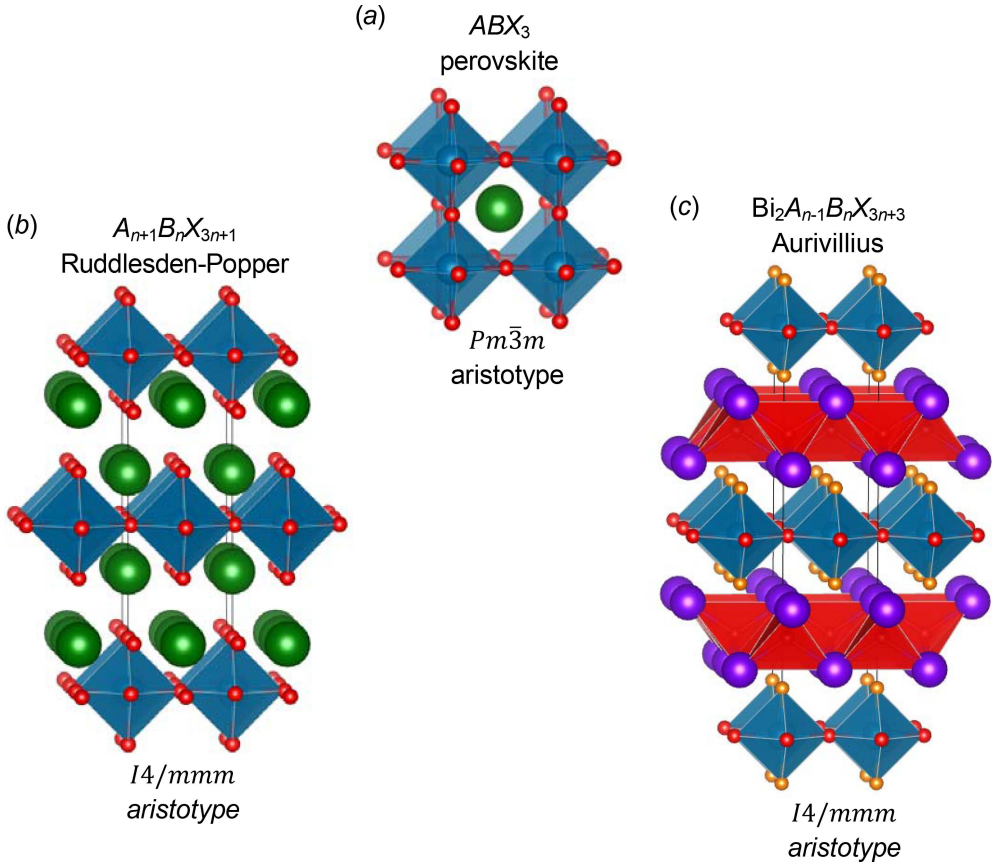

Figure 1
In this figure (*a*) shows the ideal aristotype structure of the cubic perovskite with general formula ABX_3; (*b*) shows the ideal structure of an $n = 1$ RP phase (*e.g.* Sr_2TiO_4) and (*c*) shows the aristotype structure of an $n = 1$ Aurivillius phase [*e.g.* $Bi_2TiO_4F_2$ (Needs *et al.*, 2005)]. *A*, *B* and *X* ions are shown in green, blue and red, respectively with BX_6 octahedra shown in blue and the $[Bi_2O_2]^{2+}$ fluorite-like layers in the Aurivillius structure shown in red.

1987; Hatch *et al.*, 1989) and this understanding has been key in designing complex functional materials (Pitcher *et al.*, 2015; de Araujo *et al.*, 1995; Oh *et al.*, 2015).

The hybrid analogues adopt structures with the same topology, comprising networks of corner-linked BX_6 octahedra (such as the lead halide systems), but with molecular cations on the *A* site, such as ammonium and methylammonium. The hybrid systems have similar structural degrees of freedom to the all-inorganic materials but with added complexity due to the shape and different bonding characteristics of the molecular *A* cations (Saparov & Mitzi, 2016; Mao *et al.*, 2019; McNulty & Lightfoot, 2021). Understanding the structures and symmetries of these hybrid layered perovskite-related systems, with significant dispersion forces and hydrogen bonding distinguishing them from their all-inorganic counterparts, will be key for designing optimized functional materials.

Liu *et al.* focus on the $n = 1$ RP [Fig. 1(*b*)] and their work (Liu *et al.*, 2023) will be valuable to those studying both on hybrid and all-inorganic materials. Their approach is to use the extremely powerful web-based *ISODISTORT* software (Stokes *et al.*, 2006; Stokes *et al.*, 2022) to identify the symmetry-adapted distortion modes to describe possible rotations of BX_6 octahedra about both in-plane and out-of-plane axes. The authors then determine the resulting space groups and basis vectors that allow these degrees of freedom (individual tilts and combinations of tilts). Crucially this work builds on earlier studies by including in-phase tilts about an in-plane axis [ψ tilts, in Aleksandrov notation (Aleksandrov *et al.*, 1987)]. These tabulated results alone will be an important resource for those working on the structural characterization of $n = 1$ RP (and Aurivillius) phases.

Surveying structural databases (the Cambridge Structural Database and the Inorganic Crystal Structure Database) allowed the authors to identify common structures and tilt patterns in hybrid $n = 1$ RPs and to make comparisons with the all-inorganic analogues. Their findings highlight the importance of hydrogen bonding and dispersion forces – both in explaining the relative energy scales (and therefore temperatures) of the distortions, and in understanding the different tilt patterns observed.

A key highlight for me are the findings regarding loss of inversion symmetry in these $n = 1$ materials. Both out-of-phase tilts about an in-plane axis (ϕ tilts) and tilts about an out-of-plane axis (θ tilts) do not break inversion symmetry – either alone, or in combination [as emphasized by McNulty & Lightfoot (2021)] giving centrosymmetric structures (see Table 1 in Liu *et al.*). The $n = 1$ Aurivillius phases provide all-inorganic examples of this, with the common tilt pattern $\phi\phi\theta/\phi\phi\theta$ giving centrosymmetric structures of *Pbca* symmetry:

(*a*) with only tilts [*e.g.* Bi_2NbO_5F (McCabe *et al.*, 2007)], the structure is of *Pbca* symmetry;

(*b*) additional polar displacements are needed to break inversion symmetry [*e.g.* to $Pca2_1$ symmetry with in-plane polarization as for Bi_2WO_6 (Knight, 1992, 1993) and Bi_2MoO_6 (Teller *et al.*, 1984); see also the clear discussion by McNulty & Lightfoot (2021), and the symmetry map for $Bi_2TiO_4F_2$ (Giddings *et al.*, 2021)].

This contrasts with the n = 2 RP and Aurivillius phases for which equivalent tilt patterns may break inversion symmetry (Aleksandrov & Bartolome, 1994) [*e.g.* $A_2LaTaTiO_7$ (Mallick *et al.*, 2021), $Sr_3Zr_2O_7$ (Yoshida *et al.*, 2018)].

On the other hand, if in-phase (ψ) tilts about an in-plane axis are included, inversion symmetry is often broken (see Table 2 in Liu *et al.*). There are few examples of systems including ψ tilts. The authors explain this in terms of the different cation environments that result, and suggest cation-ordering strategies to design such non-centrosymmetric systems among the hybrid n = 1 RP phases.

This systematic crystallographic study of the possible tilt combinations and structures for n = 1 RP phases will be a key reference for those working on both hybrid and on all-inorganic systems. It will be particularly exciting to see researchers apply this understanding of the molecular *A* cation bonding to realize specific tilt combinations (and symmetries) as they seek to prepare new functional materials with optimized properties.

References

Aleksandrov, K. S. & Bartolome, J. (1994). *J. Phys. Condens. Matter*, **6**, 8219–8235.

Aleksandrov, K. S. & Bartolomé, J. (2001). *Phase Transit.* **74**, 255–335.

Aleksandrov, K. S., Beznosikov, B. V. & Misyul, S. V. (1987). *Phys. Status Solidi A*, **104**, 529–543.

Araujo, C. A. de, Cuchiaro, J. D., McMillan, L. D., Scott, M. C. & Scott, J. F. (1995). *Nature*, **374**, 627–629.

Attfield, J. P., Lightfoot, P. & Morris, R. E. (2015). *Dalton Trans.* **44**, 10541–10542.

Aurivillius, B. (1950*a*). *Ark. Kemi*, **1**, 463–480.

Aurivillius, B. (1950*b*). *Ark. Kemi*, **1**, 499–512.

Aurivillius, B. (1952). *Ark. Kemi* **4**, 39–47.

Giddings, A. T., Scott, E. A. S., Stennett, M. C., Apperley, D. C., Greaves, C., Hyatt, N. C. & McCabe, E. E. (2021). *Inorg. Chem.* **60**, 14105–14115.

Glazer, A. M. (1972). *Acta Cryst.* B**28**, 3384–3392.

Hatch, D. M. & Stokes, H. T. (1987). *Phys. Rev. B*, **35**, 8509–8516.

Hatch, D. M., Stokes, H. T., Aleksandrov, K. S. & Misyul, S. V. (1989). *Phys. Rev. B*, **39**, 9282–9288.

Howard, C. J. & Stokes, H. T. (1998). *Acta Cryst.* B**54**, 782–789.

Knight, K. S. (1992). *Miner. Mag.* **56**, 399–409.

Knight, K. S. (1993). *Ferroelectrics*, **150**, 319–330.

Kojima, A., Teshima, K., Shirai, Y. & Miyasaka, T. (2009). *J. Am. Chem. Soc.* **131**, 6050–6051.

Li, T., Clulow, R., Bradford, A. J., Lee, S. L., Slawin, A. M. Z. & Lightfoot, P. (2019). *Dalton Trans.* **48**, 4784–4787.

Liu, T., Holzapfel, N. P. & Woodward, P. M. (2023). *IUCrJ*, **10**, 385–396.

Mallick, S., Fortes, A. D., Zhang, W., Halasyamani, P. S. & Hayward, M. A. (2021). *Chem. Mater.* **33**, 2666–2672.

Mao, L., Stoumpos, C. C. & Kanatzidis, M. G. (2019). *J. Am. Chem. Soc.* **141**, 1171–1190.

McCabe, E. E., Jones, I. P., Zhang, D., Hyatt, N. C. & Greaves, C. (2007). *J. Mater. Chem.* **17**, 1193–1200.

McNulty, J. A. & Lightfoot, P. (2021). *IUCrJ*, **8**, 485–513.

Megaw, H. D. (1952). *Acta Cryst.* **5**, 739–749.

Needs, R. L., Dann, S. E., Weller, M. T., Cherryman, J. C. & Harris, R. K. (2005). *J. Mater. Chem.* **15**, 2399–2407.

NREL (2023). *Best research-cell efficiency chart*, https://www.nrel.gov/pv/cell-efficiency.html.

Oh, Y. S., Luo, X., Huang, F. T., Wang, Y. Z. & Cheong, S. W. (2015). *Nat. Mater.* **14**, 407–413.

Pitcher, M. J., Mandal, P., Dyer, M. S., Alaria, J., Borisov, P., Niu, H., Claridge, J. B. & Rosseinsky, M. J. (2015). *Science*, **347**, 420–424.

Ruddlesden, S. N. & Popper, P. (1957). *Acta Cryst.* **10**, 538–539.

Ruddlesden, S. N. & Popper, P. (1958). *Acta Cryst.* **11**, 54–55.

Salje, E. K. H., Osmaston, M. F., O'Nions, R. K., Clayton, R. & Parsons, B. (1989). *Philos. Trans. R. Soc. London Ser. A*, **328**, 409–416.

Saparov, B. & Mitzi, D. B. (2016). *Chem. Rev.* **116**, 4558–4596.

Stokes, H. T., Hatch, D. M., Campbell, B. J. & Tanner, D. E. (2006). *J. Appl. Cryst.* **39**, 607–614.

Stokes, H. T., Hatch, D. M. & Campbell, B. J. (2022). *Isodistort, isotropy software suite*, https://iso.byu.edu.

Stoumpos, C. C., Cao, D. H., Clark, D. J., Young, J., Rondinelli, J. M., Jang, J. I., Hupp, J. T. & Kanatzidis, M. G. (2016). *Chem. Mater.* **28**, 2852–2867.

Teller, R. G., Brazdil, J. F., Grasselli, R. K. & Jorgensen, J. D. (1984). *Acta Cryst.* C**40**, 2001–2005.

Tsai, H. H., Nie, W. Y., Blancon, J. C., Stoumpos, C. C., Asadpour, R., Harutyunyan, B., Neukirch, A. J., Verduzco, R., Crochet, J. J., Tretiak, S., Pedesseau, L., Even, J., Alam, M. A., Gupta, G., Lou, J., Ajayan, P. M., Bedzyk, M. J., Kanatzidis, M. G. & Mohite, A. D. (2016). *Nature*, **536**, 312–316.

West, A. R. (2014). *Solid state chemistry and its applications*, 2nd ed. New York: Wiley.

Woodward, P. M. (1997). *Acta Cryst.* B**53**, 32–43.

Yoshida, S., Fujita, K., Akamatsu, H., Hernandez, O., Sen Gupta, A., Brown, F. G., Padmanabhan, H., Gibbs, A. S., Kuge, T., Tsuji, R., Murai, S., Rondinelli, J. M., Gopalan, V. & Tanaka, K. (2018). *Adv. Funct. Mater.* **28**, 1801856.